CASE STUDY OF THE THUNDERSTORM ACTIVITIES OVER NORTHERN TAIWAN DURING LATE AUGUST 1999

[1]JingShan Hong
[2]Shiung-Ming Deng and [1]Kuo-Cheng Lu

[1]*Central Weather Bureau*
[2]*Institute for Information Industry*

Abstract

The vital thunderstorm activities over one week were occurred around northern Taiwan during late August 1999. These thunderstorms were unusual severe and accompanied with the hail reports. There are two folds in this paper: first, to investigate which components of the synoptic condition, in dynamic and thermodynamic aspect, provided the storm activities over one week. The second is down to the local scale to identify the storm tracks and tries to find the relations between the storm initiation, motion, and evolution with the orography. Finally are the conclusions.

1. Synoptic overview

Figure 1 is the snapshots of GMS IR images for 26~31 Aug 1999. The figure shows that the active convection was occurred not only over Taiwan but also along the coastal region of Mainland China. The convection activities were typical summer thunderstorms and could be expected to highly correlate to the interaction between the thermal heating and local circulation which was due to the orographic effect and land-sea contrast. The convection over northern Taiwan was unusual

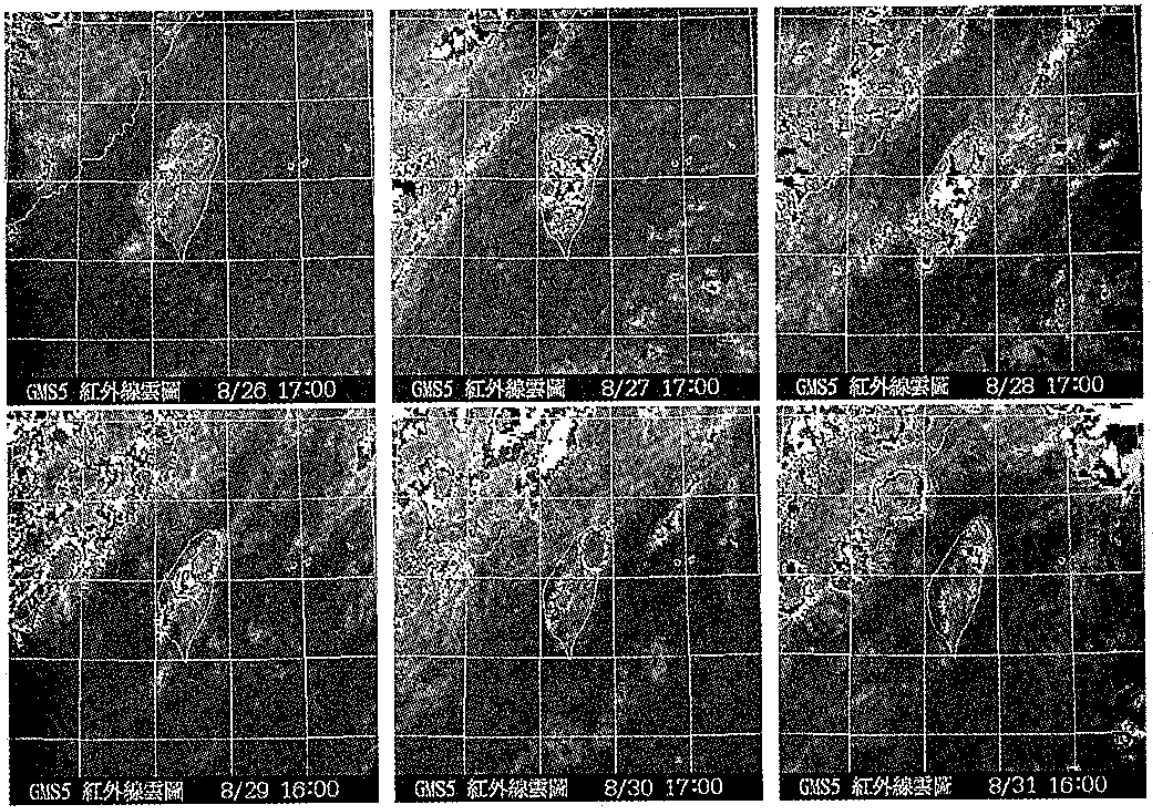

Fig. 1: The GMS IR image for 26~31 Aug 1999.

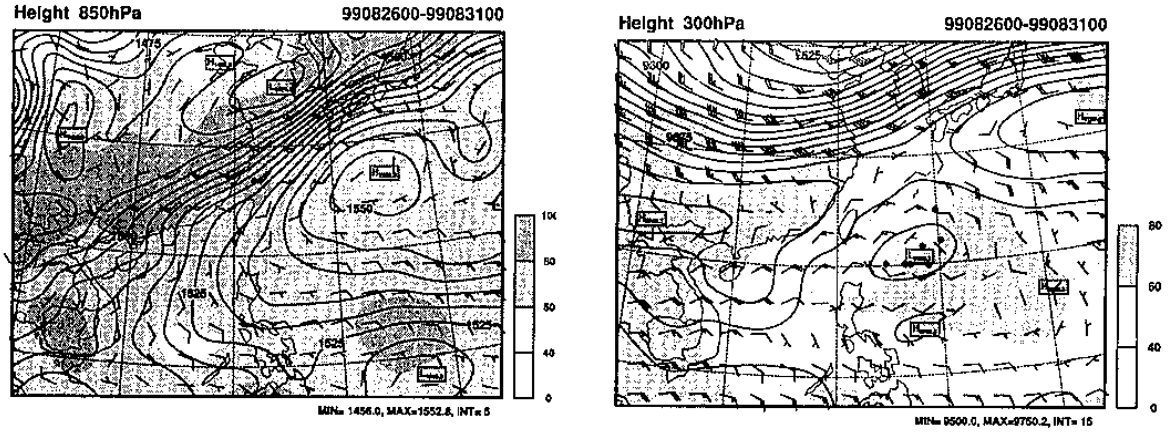

Fig. 2: The composite analysis field at 850 and 300 hPa for 26~31 Aug 1999. The solid line is height with contour intervals of 5 m at 850 hPa and 15 m at 300 hPa. Shading is the relative humidity field. The full bar of the wind flag is 5 m/s. The dots are the location of the cold core low defined by local height minimum every 12 hours at 200 hPa.

severe and accompanied several hail reports. Thus, we were interested in understanding which components of the environment provided the favor condition, in dynamic and thermodynamic aspect, to support the storm activities over one week.

Since the synoptic patterns during 26~31 Aug were quite similar, the composite filed was favorable to highlight the characteristics of the weather system during that period. Figure 2 is the composite analysis field from Limit Area Forecast System in Central Weather Bureau, from 26 to 31 Aug 1999. The figure shows that a frontal system accompanied with a prefrontal relative strong wind (10~15 m/s) was located north of Taiwan at 850 hPa. However, the frontal system had no direct influence on Taiwan. It is evident that the wind speed was less than 5 m/s and the relative humidity was only 60~80% over Taiwan area. The lower relative humidity associated with the southwest flow at 850 hPa shows that the weather was dominated by the Subtropical High. At 300 hPa, the upper level trough was still far away from Taiwan. The figure also shows that a quasi-stationary cold core low was located east of Taiwan. The associated cyclonic circulation apparently resulted in the northeastern wind component over Taiwan area.

Although the frontal system had no direct influence on Taiwan area, the anti-cyclonic shear associated with the prefrontal relative stronger wind could result in the smaller absolute vorticity and indicate the smaller inertia stability. The impact can be interpreted, without lose of generality, by the absolute vorticity on isentropic surface, say potential vorticity (PV). The inverse of PV is proportional to the Rossby radius of deformation (L_R) which is the length scale that the rotation effect becomes as important as buoyancy effect. On the other viewpoint, the time scale of the geostrophic adjustment is inversely proportional to the inertial frequency of the flow which is proportional to the PV. Thus, the flow with small PV would inhibit the geostrophic adjustment and favor the buoyancy convection. Under the circumstance, the surface heating would have the tendency to be adjusted through gravity wave and favor to trigger the convection if atmosphere is potential unstable. Thus, potential vorticity is suggested to be a quantitative measurement for the so-called "weak synoptic

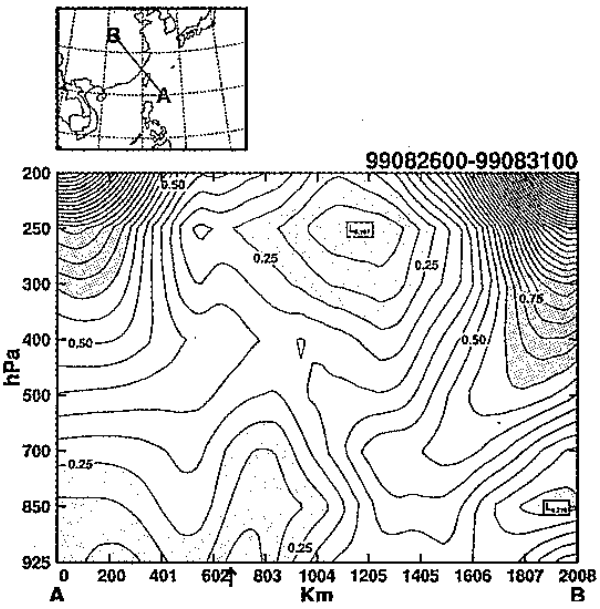

Fig. 3. The cross section of the composite potential vorticity field. The contour interval is 0.05 PVU. Light and dark shading is potential vorticity little than 0.25 and greater than 0.6 PVU, respectively. The arrow is the position of Taiwan.

forcing" for local convection.

A cross section of the composite PV field across the front was presented in Fig. 3. The low PV below 700 hPa around Taiwan area (denoted by the arrow) were dominated by the Subtropical High (0~500 km), and anti-cyclonic shear (500~1000 km) over the pre-frontal region. At upper troposphere, there were two PV maximums and a PV minimum. The PV maximum was contributed by the cold core low (south one), which was almost barotropic and only developed above 500 hPa. The other was associated with the upper level trough (the north one), which was tilted downward to the troposphere, and then coupled with the low-level frontal system. On the other hand, the local PV minimum at 250 hPa was contributed by the anti-cyclonic shear associated with the upper level trough and cold core low. As the result, areas around Taiwan and southeast Mainland China possessed a low PV characteristic in the whole deep troposphere. Thus, as mentioned, the weather pattern as shown in Fig. 3 was dynamically favorable to the convective adjustment for a given radiation heating.

Figure 4 was the time series of the sounding in Penchiao from 23~31 Aug. The atmosphere was dominated by southwest wind below 600 hPa. However, the wind speed was weak (less than 5 m/s) and lack of vertical wind shear. Though the storm activities was severe and accompanied with the hail reports, the storm dynamics inferred from the vertical shear was apparently different from the hail storm as seen in mid-West America (Weisman and Klemp 1984). Figure 4 also showed that the potential unstable layer ($\partial\theta_e/\partial z<0$) was up to 600 hPa and θ_e had the local minimum at 550 hPa. The averaged CAPE was about 1000 m^2s^2. Though the southwest flow was weak, the unstable stratification was built up and strengthened by the continuously northward advection of the moisture and warm air after 26 Aug. The cold anomaly occurred above 600 hPa after 26 Aug was possible due to the cold advection by the north wind component associated with cold core low. The cooling effect at upper level could have two extensions: first, it leaded to the local minimum of θ_e at 550 hPa after 26 Aug and then enhanced the depth and strength of potential unstable layer. Second, it lowered down the altitude of 0°C level from 5069 m at 0000 UTC 26 Aug to 4678 m at 0000 UTC 30 Aug. The descend of the 0°C level could be helpful to avoid the hails melting out before they fell down the surface.

2. Storm tracks

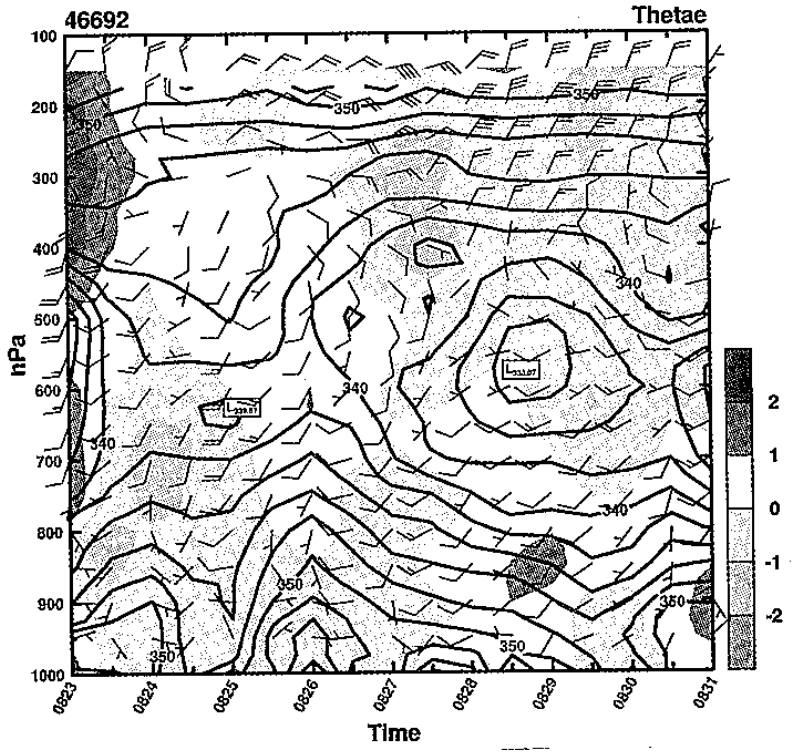

Fig. 4: Time-height plot of radiosounde observation at Panchiao. The solid line is equivalent potential temperature with interval of 2K, shading is the temperature deviation from the time mean at each level. The full bar of wind flag is 5 m/s.

Since the synoptic condition was almost steady during late Aug, the atmosphere could be served as a nature laboratory, which could generate the convection repeatedly. Thus, the storm activities during late Aug could be collected together to investigate the impact of the orography, and local circulation on the storm initiation, propagation, and evolution by using the storm track analysis.

In the paper, the storm tracks were derived from WSR-88D Doppler radar at RCWF for 26~29 and 31 Aug. All Doppler radar volumes with 10 PPI scans were completed in roughly 6 min. The cells were defined by cooperating objective and subjective processes as follows:

1. Interpolated the radar reflectivity to CAPPI with resolution of 0.5 km.
2. Created the reflectivity maximum field (CV) for the

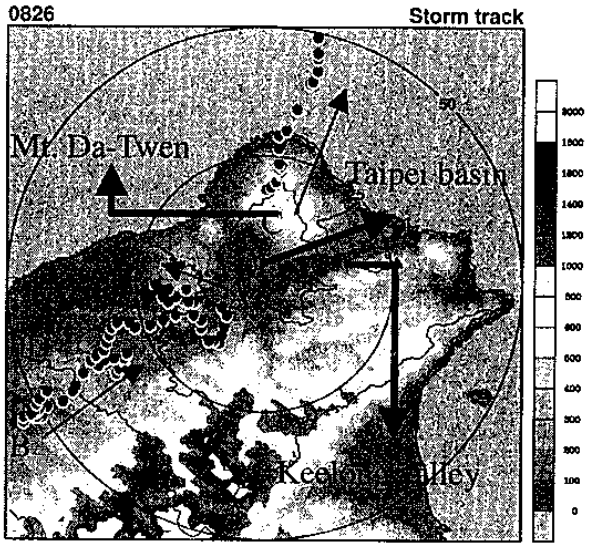

Fig. 5: The storm track for cell A (blue dots), B (red dots), C (black dots), and D (pink dots) derived from the radar reflectivity field on 26 Aug. The shading is the terrain height. Symbol ▲ denotes the position of the Doppler radar. The arrow is the direction of the storm propagation

1~3 km level.

3. Cell was defined as the area coverage of 30 dBz was greater than 25 km^2 and the location of the cell was determined as the position of the maximum value of the CV field within the cell.
4. Subjective modify was made for the possible mislead from the automatic processes 1~3. The initial and dissipated stage of the storm might not be detected by the processes 3 and was defined subjectively.

The lifetime and short remarks about the cells for all the case are given in Table 1. The table shows that, in general, the lifetime of the individual cell was usually 1~2 hours. There were four cells identified on 26 Aug and their tracks were shown in Fig. 5. Cell A, B, and D were initiated at plain where the topography was less than 500 m. Apparently, The initiation of storm C was closely related to the heating effect of the Da-Twen Mountain. All the storms, except cell A, propagated northeastward which was following the prevailing southwest wind. The initiation of the storm on 26 Aug was quite late (after 1400 LST) especially D cell which was initiated at 1752 LST.

Table 1: The lift time (in local time) and short description for the cells during 26~31 Aug 1999. The storm track of the identified cells are plotted in Figs. 5~9.

Date	cell	start	End	life time	Remark
0826	A	14:11	16:35	2:24	
	B	14:47	17:28	2:41	
	C	15:23	17:22	1:59	
	D	17:52	19:04	1:12	
0827	A	13:59	17:41	3:42	
	B	14:29	15:35	1:06	
	C	14:23	17:17	2:54	Split at 14:59, left cell die at 17:17, right cell die at 16:22
0828	A	13:03	13:45	0:42	A merge to B at 13:45
	B	13:15	14:45	1:30	B merge to C at 14:45
	C	14:21	16:09	1:48	
0829	A	12:19	13:37	1:18	
	B	13:40	15:06	1:26	B merge to C at 15:06
	C	14:00	16:48	2:48	
	D	13:54	16:18	2:24	D merge to C at 16:18
0830	NA	NA	NA	NA	NA
0831	A	12:14	14:26	2:12	
	B	13:32	14:44	1:12	
	C	14:26	16:02	1:28	Triggered by B

Three cells were defined on 27 Aug and the tracks were shown in Fig 6. A and B cell were triggered at steeper terrain slope about 500~1000 m and tended to be stationary. Again, initiation of C cell was closely related to Da-Twen Mountain. The initial time of cells on 27 Aug was slightly earlier than 26 Aug but still late (after 1400 LST). Cell splitting was occurred for cell C at 1459 LST. Left cell was weaker, propagated roughly down the Keelong valley, and then dissipated over ocean. Right cell propagated up slope and was stronger than left one. The maximum reflectivity of right cell was up to 57 dBz.

Initiation of convection on 28 Aug was, in general, after 1300 LST and much earlier than before. It may be due to the more unstable stratification after 28 Aug as shown in Fig. 4. A and B cells were triggered at the mountain peak but weaker (Fig. 7). Cell merge was occurred that A merged to B at 1345 LST and B merged to C at 1445 LST. C cell was initiated at mountain slope, propagated down slope, accelerated when passing Taipei basin area, and then dissipated as the storm encountered the Da-Twen Mountain. C cell had the maximum reflectivity up to 63 dBz as it passed

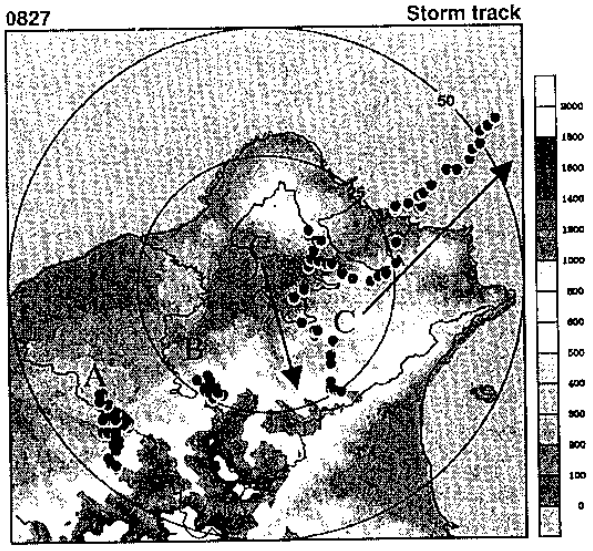

Fig. 6: Same as Fig. 5 but for 27 Aug.

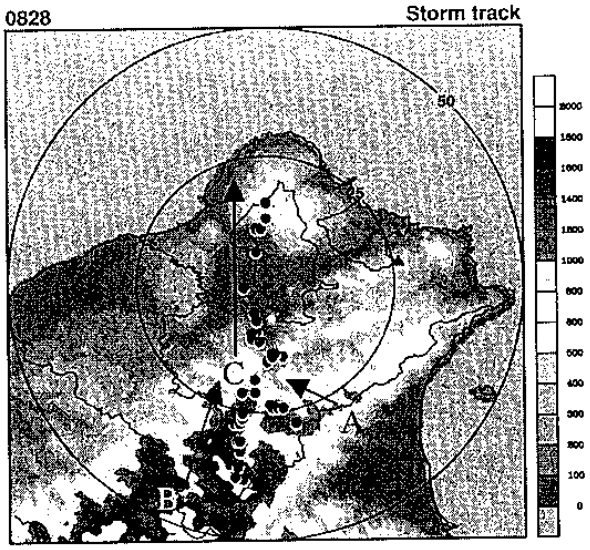

Fig. 7: Same as Fig. 5 but for 28 Aug.

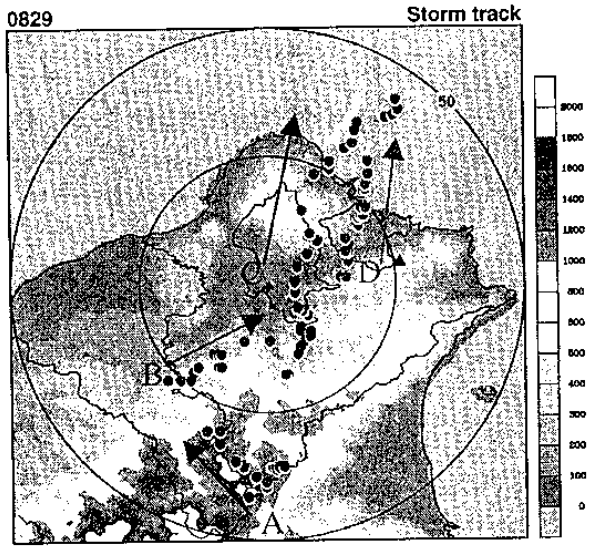

Fig. 8: Same as Fig. 5 but for 29 Aug.

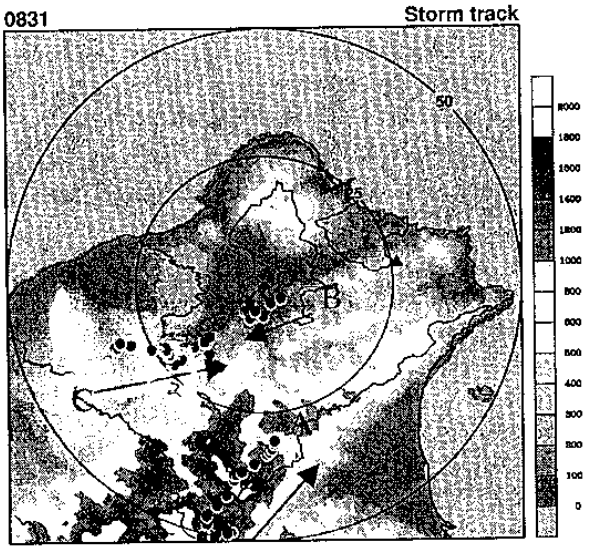

Fig. 9: Same as Fig. 5 but for 31 Aug.

through Taipei basin area. After the cell reached the maximum reflectivity, the storm was dissipated in 40 minutes

Tracks for four cells on 29 Aug are shown in Fig. 8. Cell A was the first detectable cell at 1219 LST and initiated on mountain peak. The other three cells were triggered on terrain slope or foothill and initiated later than A cell. There was no significant movement for A cell. B, C, and D cell propagated down the prevailing wind. B and D cell merged to C cell at 1506 LST and 1618 LST, respectively. The strongest reflectivity was 63 dBz as C cells traveling over Taipei basin area. The initiation and the propagation of B and C cell were similar to the case as shown in Jou (1994) and Chen and Chan (1994).

Figure 9 shows that cell A was triggered on mountain peak (1214 LST) and was earlier than the other two cells on 31 Aug. Cell B was the only one cell for all the collective cells that initiated over basin area. Though the lifetime of cell B was quite short, the cell reached its maximum reflectivity up to 60 dBz. Cell C was triggered by Cell B and propagated westward.

3. Discussion and conclusions

Continuous thunderstorm activities were occurred over one week around northern Taiwan during late August 1999. This paper analyzed the composite environmental condition during the period and tried to interpret the roles of the weather

systems on local storm activities via dynamic and thermodynamic viewpoint. By the way, we were also down to the local scale to identify the storm tracks and try to find the relations between the storm activities, motion, and evolution with the orography.

The environmental conditions were described as follows:

1. Taiwan was dominated by the Subtropical High and located on the anti-cyclonic shear side of the low level strong wind which was associated with the front system at 850 hPa.
2. The vertical wind shear over Taiwan area was quite weak.
3. The frontal system and upper level trough was far way from Taiwan. However, the cold core low at upper troposphere, which was nearly stationary from 26 to 31 Aug, was located to the east of Taiwan

The roles of the weather system on the local convective activities were interpreted as follows:

1. Taiwan was located at the anti-cyclonic shear side both in the lower and upper troposphere. The anti-cyclonic shear contributed to the low potential vorticity within the whole troposphere around Taiwan and southeastern Mainland China and was favor to the local convective activities.
2. Potential vorticity is suggested to be a quantitative measurement for the so-called "weak synoptic forcing" for local convection.
3. The unstable stratification was built up and strengthened by the continuously northward advection of the moisture and warm air after 26 Aug though the southwest flow was quite weak. On the other hand, The west branch of cold core low advected the relative cold/dry air southward and then increased the local thermal instability.
4. The cold advection at upper level lowered down the altitude of 0°C level. The descend of the 0°C level could be helpful to avoid the hails melting out before they fell down the surface.

The track analysis was summarized:

1. The convection was initiated, in general, after 1400 LST on 26~27 Aug, which was later than 28~31 Aug. This might be related to the increase of the unstable stratification after 28 Aug.
2. The storms initiated on mountain peak were earlier and the strength was weaker than those on plain or terrain slope. This could be interpreted as follows. The convergence over mountain peak could be generated by the symmetric up slope wind across the mountain due to the solar heating. Such a convergence was favor to trigger the convection efficiently. However, the convection was expected to be weaker because of the deficiency in moisture supplement. On the other hand, in general, the coupling of up slope wind and sea breeze was necessary to produce the enough convergence to trigger the convection at plain or terrain slope. It might take longer time to build up the sea breeze circulation and the up slope wind over more frank topography so that the initiation of the storm would be later than those on mountain peak. However, The storm was usually stronger because the moisture could be supplied by the sea breeze.
3. The storm initiated on the mountain peak tends to be stationary, or only propagate over the mountain peak area. The convection on terrain slope or plain usually propagated down the prevailing wind.
4. Da-Twen Mountain played the role to trigger the local convection due to the surface heating.
5. Despite the steering from prevailing wind, the propagation of the storm seemed to be sensitive to the orography, e.g. blocking by the Da-Twen Mountain or guiding by the Keelong valley.
6. Storm splitting, merging, and triggered by the old cells were a common features.
7. The lifetime of the storm was ordinary (1~2 hours) but the convection was rather severe. The maximum reflectivity was usually up to 60 dBz and then dissipated very soon as it reached its maximum reflectivity.

The storm track analysis could provide useful information for model simulation to further study the impact of the orography and local circulation on summer thunderstorm in Taiwan area. By the way, the climatology of the storm track was also useful for the nowcasting.

Reference

Chen, C. S., and Y. E. Chan, 1994: On the formation of cloud and precipitation systems in Taiwan during TAMEX IOP #11. *T. A. O.*, **5**, 137 - 168.

Jou, B. J.-D., 1994: Mountain-originated mesoscale precipitation system in northern Taiwan: a case study 21 June 1991. *T. A. O.*, **5**, 169 - 199.

Weisman, M. L., and J. B. Klemp: 1984: The structure and classification of numerically simulated convective storms in directionally varying wind shears. *Mon. Wea. Rev.*, **112**, 2479 - 2498.